The Journal of Experimental Biology 210, 2714-2722
Published by The Company of Biologists 2007
doi:10.1242/jeb.004507

# Flight stabilization control of a hovering model insect

Mao Sun* and Ji Kang Wang

*Institute of Fluid Mechanics, Beijing University of Aeronautics and Astronautics, Beijing 100083, People's Republic of China*

*Author for correspondence (e-mail: m.sun@263.net)

*Accepted 7 May 2007*

## Summary

**The longitudinal stabilization control of a hovering model insect was studied using the method of computational fluid dynamics to compute the stability and control derivatives, and the techniques of eigenvalue and eigenvector analysis and modal decomposition, for solving the equations of motion (morphological and certain kinematical data of hoverflies were used for the model insect).**

**The model insect has the same three natural modes of motion as those reported recently for a hovering bumblebee: one unstable oscillatory mode, one stable fast subsidence mode and one stable slow subsidence mode. Controllability analysis shows that although unstable, the flight is controllable. For stable hovering, the unstable oscillatory mode needs to be stabilized and the slow subsidence mode needs stability augmentation. The former can be accomplished by feeding back pitch attitude, pitch rate and horizontal velocity to produce $\delta\bar{\phi}$ or $\delta\alpha_2$; the latter by feeding back vertical velocity to produce $\delta\Phi$ or $\delta\alpha_1$ ($\delta\Phi$, $\delta\bar{\phi}$, $\delta\alpha_1$ and $\delta\alpha_2$ denote control inputs: $\delta\Phi$ and $\delta\bar{\phi}$ represent changes in stroke amplitude and mean stroke angle, respectively; $\delta\alpha_1$ represents an equal change whilst $\delta\alpha_2$ a differential change in the geometrical angles of attack of the downstroke and upstroke).**

Key words: insect, hovering, flight controllability, stabilization control, Navier–Stokes simulation, modal analysis.

## Introduction

Recently, with the current understanding of the aerodynamic force mechanisms of insect flight, researchers are beginning to devote more effort to the area of flight dynamics (e.g. Taylor and Thomas, 2003; Sun and Xiong, 2005).

Taylor and Thomas studied dynamic flight stability in the desert locust *Schistocerca gregaria* at forward flight (Taylor and Thomas, 2003). In the study, they employed the 'rigid body' assumption. That is, the insect was treated as a rigid flying body with only 6 degrees of freedom and the effects of the flapping wings on the flying body being represented by the wing beat cycle average forces and moments that could vary with time over the time scale of the insect body. The linear theory of aircraft flight dynamics was applied to the analysis. They first measured the aerodynamic force and moment variations of the tethered locust by varying the wind-tunnel speed and the attitude of the insect, obtaining the aerodynamic derivatives. Then they studied the longitudinal dynamic flight stability of the insect using the techniques of eigenvalue and eigenvector analysis, and showed that the disturbed motion consisted of three natural modes of motion: one stable subsidence mode, one unstable divergence mode and one stable oscillatory mode. It should be noted that their experimental approach, using real insects (Taylor and Thomas, 2003), necessarily included some control responses, and the aerodynamic derivatives they measured are not the inherent (or passive) stability derivatives, but stability derivatives with some control effects. Sun and Xiong studied the dynamic flight stability of a bumblebee at hovering flight (Sun and Xiong, 2005). They also employed the rigid body approximation and the linear theory, but unlike Taylor and Thomas, these authors obtained the aerodynamic derivatives using the method of computational fluid dynamics (CFD). The computational approach allows simulation of the inherent stability of a flapping motion in the absence of active control, which is difficult to achieve in experiments using real insects. They showed that the longitudinal disturbed motion of the hovering bumblebee consisted of an unstable oscillatory mode, a stable fast subsidence mode and a stable slow subsidence mode.

Due to the existence of the unstable modes, the hovering flight of the bumblebee (Sun and Xiong, 2005) and the forward flight of the desert locust (Taylor and Thomas, 2003) are inherently unstable. When the flight of an insect is inherently unstable, in order to achieve stable flight the insect must stabilize the flight by constantly moving its controls. In fact, one of the functions of insect control systems is to provide stability (Dudley, 2000; Taylor, 2001). Deng et al. presented a design of the flight control algorithms for biomimetic robotic insects (Deng et al., 2006). The system matrix of locust flight in Taylor and Thomas (Taylor and Thomas, 2003) was recently modified by adding a moment derivative (with respect to pitch angle) to the matrix and showing that the unstable model of locust flight could be stabilized by feeding back the pitch attitude to produce a pitch moment (Taylor et al., 2006). There has not, however,

been any formal quantitative study on stabilization control of insect flight based on stability and controllability analysis (controllability is a property of the coupling between the control input and the motion; see Materials and methods).

In the present study, we conduct a formal quantitative analysis on the stability and controllability and the stabilization control of the hovering flight of a model insect, using the techniques based on the linear theories of stability and control. Morphological and certain kinematical data of hoverflies in hover flight are used for the model insect. We chose the data of hoverflies for two reasons. First, hoverflies conduct motionless hovering; in an almost motionless hovering flight, deviations from the equilibrium state and the applied controls must be small quantities, so linear theories can be used. Second, predictions of a model should be tested by experimental observations; hoverflies display long-term motionless hovering, both in the wild and under laboratory conditions, and using hoverfly data for our model could make future experiments easier. As a first step, we consider longitudinal motion. We first use the CFD method to compute the flows and obtain the stability and control derivatives; and then we use the techniques of eigenvalue and eigenvector analysis and modal decomposition to study the stabilization control of the hovering insect.

## Materials and methods

### *Equations of motion*

Let $oxyz$ be a non-inertial coordinate system fixed to the body and $o_Ex_Ey_Ez_E$ be an inertial coordinate system fixed to the earth (Fig. 1). The origin $o$ is at the center of mass of the insect and the axes are aligned so that the $x$-axis is horizontal and points forward at equilibrium. The variables that define the motion (Fig. 1) are the forward ($u$) and dorso-ventral ($w$) components of velocity along $x$- and $z$-axes, respectively, the pitching angular velocity around the center of mass ($q$), and the pitch angle between the $x$-axis and the horizontal ($\theta$). The $x$- and $z$-components of the total aerodynamic force are denoted as $X$ and $Z$, respectively, and the aerodynamic pitching moment is denoted as $M$ (note that they are wing beat cycle average quantities); the mass of the insect, the gravitational acceleration and the moment of inertia about the $y$ axis are denoted as $m$, $\boldsymbol{g}$ and $I_y$, respectively. The equations of motion have been given previously (Sun and Xiong, 2005; Taylor and Thomas, 2003), and also their derivation (Taylor and Thomas, 2003). We have non-dimensionalized the equations by using $c$, $U$ and $t_w$ as the reference length, speed and time ($c$ is the mean chord length of wing; $U$ is the mean flapping velocity defined as $U=2\Phi nr_2$, where $\Phi$ is the flapping amplitude, $n$ the flapping frequency, and $r_2$ the radius of second moment of wing area; $t_w$ is the wing beat period, $t_w=1/n$). The non-dimensional equations are:

$$\begin{bmatrix} \delta\dot{u}^+ \\ \delta\dot{w}^+ \\ \delta\dot{q}^+ \\ \delta\dot{\theta} \end{bmatrix} = \mathbf{A}\begin{bmatrix} \delta u^+ \\ \delta w^+ \\ \delta q^+ \\ \delta\theta \end{bmatrix} + \mathbf{Bc}\,, \tag{1}$$

where $\mathbf{A}$ is the system matrix:

$$\mathbf{A} = \begin{bmatrix} X_u^+/m^+ & X_w^+/m^+ & X_q^+/m^+ & -g^+ \\ Z_u^+/m^+ & Z_w^+/m^+ & Z_q^+/m^+ & 0 \\ M_u^+/I_y^+ & M_w^+/I_y^+ & M_q^+/I_y^+ & 0 \\ 0 & 0 & 1 & 0 \end{bmatrix}, \tag{2}$$

where the superscript '+' denotes the non-dimensional quantity; $X_u^+$, $X_w^+$, $X_q^+$, $Z_u^+$, $Z_w^+$, $Z_q^+$, $M_u^+$, $M_w^+$ and $M_q^+$ are the stability derivatives; '.' represents differentiation with respect to time; the symbol $\delta$ denotes a small disturbance quantity relative to the equilibrium value; the non-dimensional forms are: $\delta u^+=\delta u/U$, $\delta w^+=\delta w/U$, $\delta q^+=\delta q t_w$; $X^+=X/0.5\rho U^2S_t$, $Z^+=Z/0.5\rho U^2S_t$, $M^+=M/0.5\rho U^2S_t c$; $t^+=t/t_w$, $m^+=m/0.5\rho US_t t_w$ ($\rho$ denotes the air density and $S_t$ denotes the area of two wings), $I_y^+=I_y/0.5\rho U^2S_t ct_w^2$ and $\boldsymbol{g}^+=\boldsymbol{g}t_w/U$ (using the flight data given below, $m^+$, $I_y^+$ and $\boldsymbol{g}^+$ are computed as $m^+=64.24$, $I_y^+=11.65$, $\boldsymbol{g}^+=0.0227$, where $\rho$ is 1.23 kg m$^{-3}$ and $\boldsymbol{g}$ is 9.81 m s$^{-2}$).

**Bc** in Eqn 1 represents the control forces and moments; **c** is the vector of control inputs; **B** is the control system matrix, which contains the control derivatives [in the stability analyses, **Bc** was set to zero (Sun and Xiong, 2005; Taylor and Thomas, 2003)]. It has been observed that freely flying hoverflies and many other insects control the longitudinal motion mainly by changes in geometrical angles of attack and changes in the fore/aft extent of the flapping motion (Ellington, 1984b). The geometrical angle of attack in the downstroke translation is denoted by $\alpha_d$ and in the upstroke translation by $\alpha_u$. The extent of fore/aft flapping motion is determined by the stroke amplitude ($\Phi$) and the mean stroke angle ($\bar{\phi}$). On the basis of the above and other observations (e.g. Willmott and Ellington, 1997; Dudley and Ellington, 1990), it is reasonable to assume the following control input vector:

$$\mathbf{c} = \begin{bmatrix} \delta\Phi \\ \delta\alpha_1 \\ \delta\bar{\phi} \\ \delta\alpha_2 \end{bmatrix}, \tag{3}$$

where $\delta\Phi$ and $\delta\bar{\phi}$ represent changes in $\Phi$ and $\bar{\phi}$ from their respective equilibrium values; $\delta\alpha_1$ represents an equal change

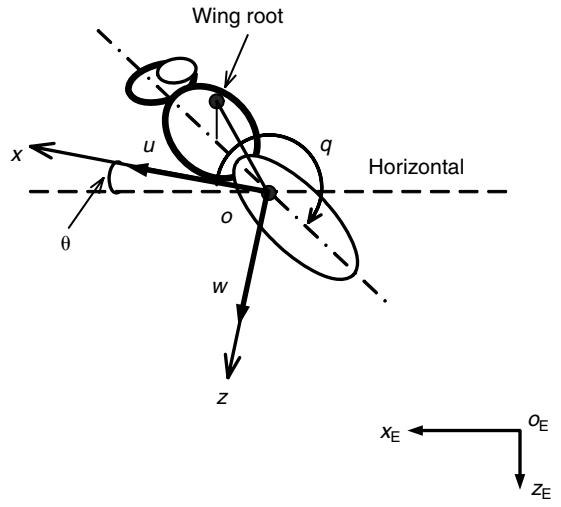


Fig. 1. Definition of the state variables $u$, $w$, $q$ and $\theta$ and sketches of the reference frames. The model insect is shown during a perturbation ($u$, $w$, $q$ and $\theta$ are zero at equilibrium).

in $\alpha_d$ and $\alpha_u$ from their respective equilibrium values (e.g. $\delta\alpha_1$=5° means that $\alpha_d$ and $\alpha_u$ both increase by 5° from their equilibrium values, respectively); $\delta\alpha_2$ represents a differential change in $\alpha_d$ and $\alpha_u$ (e.g. $\delta\alpha_2$=5° means that $\alpha_d$ increases and $\alpha_u$ decreases by 5° from their equilibrium values, respectively). With **c** defined as in Eqn 3, the control system matrix can be written as:

$$\mathbf{B} = \begin{bmatrix} X_\Phi^+/m^+ & X_{\alpha_1}^+/m^+ & X_{\bar\Phi}^+/m^+ & X_{\alpha_2}^+/m^+ \\ Z_\Phi^+/m^+ & Z_{\alpha_1}^+/m^+ & Z_{\bar\Phi}^+/m^+ & Z_{\alpha_2}^+/m^+ \\ M_\Phi^+/I_y^+ & M_{\alpha_1}^+/I_y^+ & M_{\bar\Phi}^+/I_y^+ & M_{\alpha_2}^+/I_y^+ \\ 0 & 0 & 0 & 0 \end{bmatrix}, \quad (4)$$

where $X_\Phi^+$, $X_{\alpha 1}^+$ etc. are the control derivatives.

### *Flight data*

We use the morphological and certain kinematical data of hoverflies in hover flight for the model insect. The general morphological data are as follows (Ellington, 1984a): $m$=27.3 mg; wing length ($R$) is 9.3 mm; mean chord length of wing ($c$) is 2.2 mm, radius of second moment of wing area ($r_2$) is 0.578$R$; area of one wing ($S$) is 20.46 mm$^2$; free body angle ($\chi_0$) is 53°; body length ($l_b$) is 1.10$R$; distance from wing base axis to center of mass ($l_1$) is 0.14$l_b$; pitching moment of inertia of the body about wing-root axis ($I_b$) is $2.4\times10^{-10}$ kg m$^2$ [the pitching moment of inertia about $y$-axis ($I_y$) can be computed as $I_y=I_b-l_1^2m=1.84\times10^{-10}$ kg m$^2$]. Available wing-kinematic data at equilibrium flight are: $\Phi$=90°; wing beat frequency ($n$) is 160 Hz; flip duration is approximately 25% of wingbeat cycle; stroke plane angle ($\beta$) is approximately zero; body angle ($\chi$) is 43° (Ellington, 1984b). Values of $\alpha_d$, $\alpha_u$ and $\bar\Phi$ at equilibrium flight are also needed, and they will be determined below.

### *Determination of equilibrium conditions and stability and control derivatives*

#### *The wings, the flapping motion and the flow solution method*

In determining the equilibrium conditions of the flight, we only need to calculate the flows around the wings (at equilibrium the body does not move and it is assumed that the wings and body do not interact aerodynamically). For the same reason, we only need to calculate the flows around the wings in determining the control derivatives. To obtain the stability derivatives, in principle we need to compute the flows around the wings and the body. But near hovering, as discussed previously (Sun and Xiong, 2005), the aerodynamic forces and moments of the body are negligibly small compared to those of the wings, because the velocity of the body is very small. Therefore, in estimating the aerodynamic derivatives, we still only need to compute the flows around the wings. We further assume that the contralateral wings do not interact aerodynamically. As a result, in the present CFD model, the body is neglected and the flows around the left and right wings are computed separately. The wing planform is the same as that of a hoverfly (Fig. 2), given by Ellington (Ellington, 1984a). The wing section is assumed to be a flat plate with rounded leading and trailing edges, the thickness of which is 3% of the mean chord length of the wing.

The flapping motion of the wing is assumed to consist of translation (azimuthal rotation) and flip rotation. The flapping motion has previously been described in detail (Sun and Xiong, 2005); as discussed there, $\Phi$, $n$, $\alpha_d$, $\alpha_u$, $\bar\Phi$ and flip duration must be given for prescribing the flapping motion.

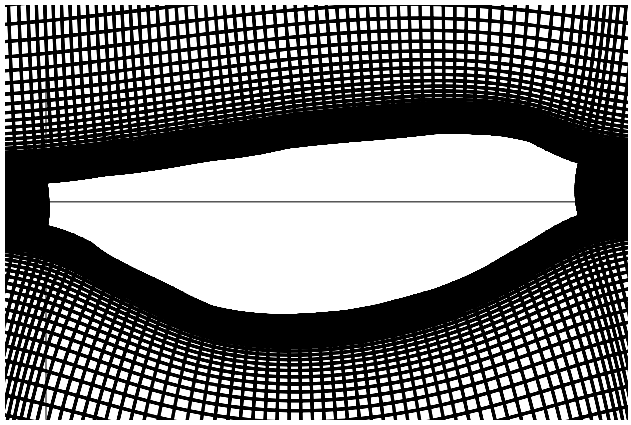

Fig. 2. Portions of the grid for the hoverfly wing.

The flow equations and the solution method used are the same as those previously described (Sun and Tang, 2002; Sun and Xiong, 2005). The computational grid has dimensions 93×109×78 in the normal direction, around the wing section and in the spanwise direction, respectively. The normal grid spacing at the wall was 0.0015. The outer boundary was set at 20 chord lengths from the wing. The time step was 0.02. A detailed study of the numerical variables such as grid size, domain size, time step, etc., was conducted and it was shown that the above values for the numerical variables were appropriate for the calculations.

#### *Equilibrium flight conditions*

As mentioned above, values of $\alpha_d$, $\alpha_u$ and $\bar\Phi$ at equilibrium flight are not available from measured data. They are determined by calculation using the force and moment balance requirements: the mean vertical force of the wings equals to insect weight and the mean horizontal force and mean pitching moment (about the mass center) of the wings equal to zero.

#### *Stability and control derivatives*

Conditions in the equilibrium flight are taken as the reference conditions in the calculation of the stability and control derivatives. By definition, a stability derivative is a partial derivative, e.g. $M_u$ represents the rate of change of $M$ when only $u$ is changed. In order to obtain the stability derivatives, similar to the case of the bumblebee (Sun and Xiong, 2005), we make three consecutive flow computations in which $u$, $w$ and $q$ are varied separately; using the computed data, curves representing the variation of the aerodynamic forces and moments with each of the $u$, $w$ and $q$ variables are fitted; the partial derivatives are then estimated by taking the local tangent (at equilibrium) of the fitted curves. Similarly, in order to obtain the control derivatives, we make four consecutive flow computations in which $\delta\Phi$, $\delta\bar\Phi$, $\delta\alpha_1$ and $\delta\alpha_2$ are varied separately. The partial derivatives are then estimated in the same way as in the case of stability derivatives.

*Method of analysis*

After the stability and control derivatives are computed, the elements of the system matrix **A** and control matrix **B** in Eqn 1 become known, and the equation now can be used to study the properties of the disturbance motion of the hovering insect. Here, we are interested in the properties of dynamic stability, controllability and stabilization control of the hovering insect.

Dynamic stability is an inherent property of the system. It deals with the motion of a flying body about its equilibrium state following a disturbance, without active control being applied (it involves the solution of Eqn 1 without the term **Bc**); if the amplitude of the oscillation decreases with time and goes to zero, then flight is dynamically stable, otherwise it is unstable or neutrally stable. The results of stability analysis could show whether or not the system needs to be controlled. Stability properties (stable or unstable; how and how fast the disturbance decrease or increase, etc.) can be determined using the techniques of eigenvalue and eigenvector analysis [this has been done for hovering bumblebee (Sun and Xiong, 2005) and for locusts in forward flight (Taylor and Thomas, 2003)]. In eigenvalue and eigenvector analysis [for a concise description of the theory, see Taylor and Thomas (Taylor and Thomas, 2003)], the disturbance motion is expressed as a linear contribution of natural modes of motion of the system, thus the stability properties of the flight can be represented by the natural modes of motion. In the present study, the technique of eigenvalue and eigenvector analysis is applied to Eqn 1 (with **Bc** set to zero). The results would tell us which mode is unstable or weakly stable (although stable, the disturbance goes to zero slowly) and needs to be controlled. In addition, the eigenvector of a natural mode of motion would tell us what are the main variables in the mode; this information is very useful in studying the control of this mode.

Controllability is a property of the coupling between the control input and the motion (and thus involves the matrices **A** and **B** in Eqn 1). A linear system is said to be controllable at time $t_0$ if there exist some input $\mathbf{c}(t)$ that makes the disturbance zero at some finite time $t_1$ ($t_1>t_0$). As discussed above, the disturbance motion can be represented by a linear combination of the natural modes of motion. Thus knowing the controllability of each of the modes gives the controllability of the flight. For each of the modes, one wishes to know if it is controllable, and (if is), which control inputs are effective for the control. This can be done using the modal decomposition method. In this method, a linearly dynamic system is transformed into modal coordinates. When the system is in modal coordinates one can immediately see which modes are controlled by which controls. A summary of the modal decomposition method can be found elsewhere (Stevens and Lewis, 2003) (see also Bryson, 1994). The modal decomposition method is used in the present study to investigate the controllability properties.

After conducting the stability and controllability analyses, the results from these analyses are combined to yield insights into the stabilization control of the hovering model insect.

## Results and analysis

*The equilibrium flight and the stability and control derivatives*

Values of $\alpha_d$, $\alpha_u$ and $\bar{\phi}$ at equilibrium flight are not provided by measured data and are determined by calculation using the force and moment balance requirements. The calculation proceeds as follows. A set of values for $\alpha_d$, $\alpha_u$ and $\bar{\phi}$ is guessed; the flow equations are solved and the corresponding mean vertical force ($Z_e^+$), mean horizontal force ($X_e^+$) and mean moment ($M_e^+$) are calculated. If $-Z_e^+$ is not equal to 1.46 (the non-dimensional weight), or $X_e^+$ not equal to zero, or $M_e^+$ not equal to zero, $\alpha_d$, $\alpha_u$ and $\bar{\phi}$ are adjusted; the calculations are repeated until the magnitudes of difference between $-Z_e^+$ and 1.46, between $X_e^+$ and 0 and between $M_e^+$ and 0 are <0.01. The calculated results show that when $\alpha_d$=33°, $\alpha_u$=33° and $\bar{\phi}$=2.4°, the equilibrium requirements are approximately met. The calculated angles of attack at equilibrium compare favorably with those estimated by Ellington (Ellington, 1984b), based on his high-speed motion picture. For readers' reference, the time courses of the vertical ($C_V$) and horizontal ($C_H$) force coefficient and pitching moment coefficient ($C_M$) at equilibrium are shown in Fig. 3 [the non-dimensional mean forces and moment ($X_e^+$, $Z_e^+$ and $M_e^+$) are obtained by taking time average of the corresponding time courses over a stroke cycle]. Note that at equilibrium, $\alpha_d$ and $\alpha_u$ of the model hoverfly are the same (33°); this is because the stroke plane is horizontal ($\beta$=0). For the bumblebee study (Sun and Xiong, 2005), $\alpha_d$ (27°) and $\alpha_u$ (21°) are different by a few degrees;

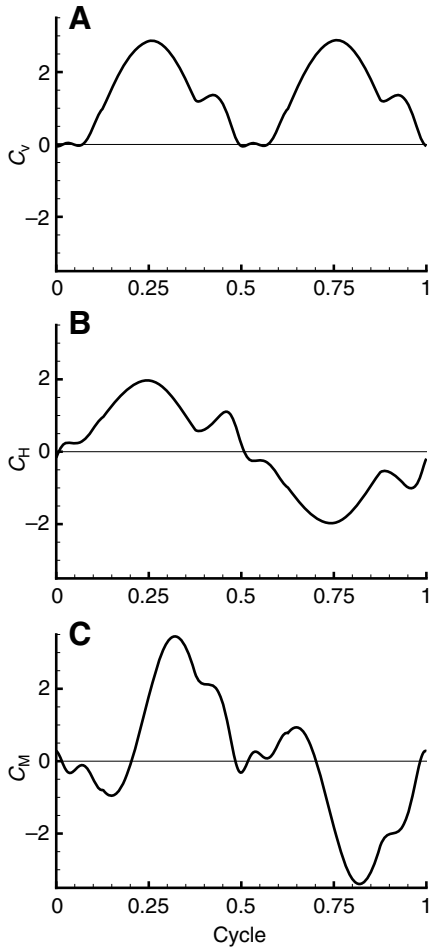


Fig. 3. (A) Time courses of vertical force coefficient ($C_v$), (B) horizontal force coefficient ($C_H$) and pitching moment coefficient ($C_M$) in one wingbeat cycle at equilibrium.

Table 1. *Non-dimensional stability derivatives*

| $X_u^+$ | $Z_u^+$ | $M_u^+$ | $X_w^+$ | $Z_w^+$ | $M_w^+$ | $X_q^+$ | $Z_q^+$ | $M_q^+$ |
|---|---|---|---|---|---|---|---|---|
| –1.28 | –0.04 | 2.32 | 0.01 | –1.26 | 0.05 | –0.28 | 0 | –0.03 |

$X_u^+$, $Z_u^+$ and $M_u^+$, non-dimensional derivatives of the *x*- and *z*-component of the aerodynamic force and aerodynamic moment, respectively, with respect to the *x*-component ($u^+$) of the non-dimensional velocity; $X_w^+$, $Z_w^+$ and $M_w^+$, non-dimensional derivatives of the *x*- and *z*-component of the aerodynamic force and aerodynamic moment, respectively, with respect to the *z*-component ($w^+$) of the non-dimensional velocity; $X_q^+$, $Z_q^+$ and $M_q^+$, non-dimensional derivatives of the *x*- and *z*-component of the aerodynamic force and aerodynamic moment, respectively, with respect to the non-dimensional pitching rate ($q^+$).

this is because its stroke plane tilts forward by a small angle ($\beta$=6°).

After the equilibrium flight conditions have been determined, flows for each of *u*, *w* and *q* varying independently from the equilibrium value are computed. The corresponding $X^+$, $Z^+$ and $M^+$ are obtained; the data are plotted in Fig. 4. The aerodynamic derivatives estimated using the *u*-series, *w*-series and *q*-series data are shown in Table 1. For the model insect, similar to the bumblebee studied (Sun and Xiong, 2005), $M_u^+$ is positive and very large, $X_u^+$ and $Z_u^+$ are negative and have relatively large magnitude, and $Z_u^+$, $X_w^+$, $M_w^+$, $X_q^+$, $Z_q^+$ and $M_q^+$ have relatively small magnitude.

Next, flows for each of the control inputs varying independently from the equilibrium value are computed. In Fig. 5, the $\Phi$-series, $\alpha_1$-series, $\bar{\phi}$-series and $\alpha_2$-series data are plotted. The control derivatives, estimated using these data, are shown in Table 2. It is seen that varying $\Phi$ or $\alpha_1$ mainly produces change in vertical force, varying $\bar{\phi}$ mainly produces change in pitching moment, and varying $\alpha_2$ mainly produces changes in horizontal force.

*Dynamic stability and the natural modes of motion*

For stability analysis, no control is applied. **Bc** in Eqn 1 is set as zero. **A** in Eqn 1 is:

$$\mathbf{A} = \begin{bmatrix} -0.0199 & 0.0002 & -0.0044 & -0.0227 \\ -0.0006 & -0.0196 & 0 & 0 \\ 0.1991 & 0.0043 & -0.0026 & 0 \\ 0 & 0 & 1 & 0 \end{bmatrix} \quad (5)$$

(the elements of **A** are computed using the stability derivatives in Table 1 and the values of $m^+$ and $I_y^+$ given above). The

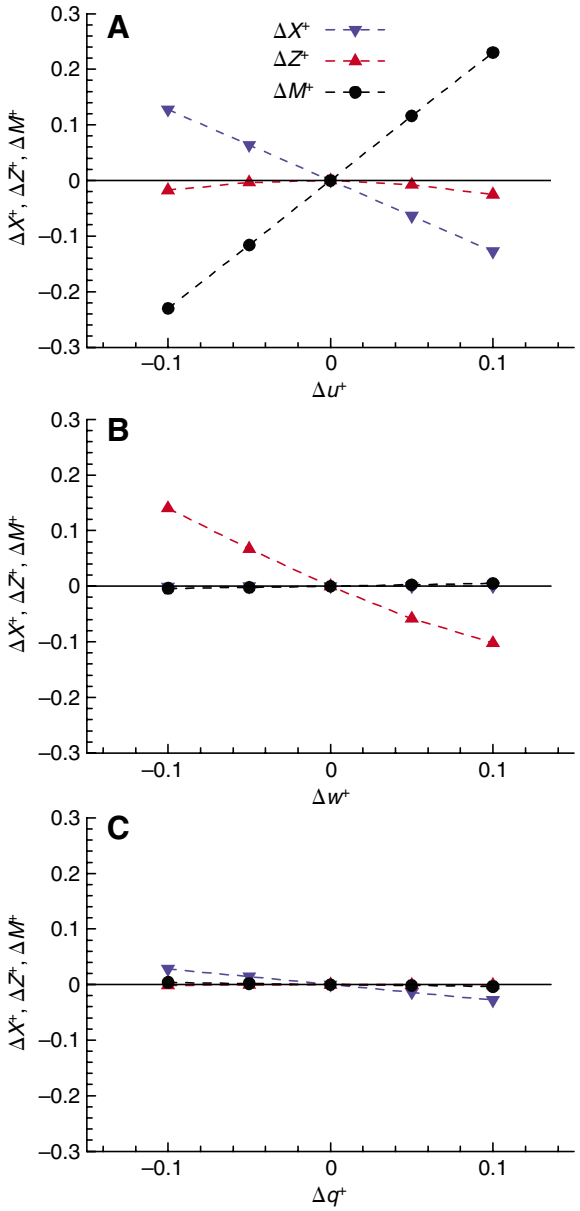


Fig. 4. The *u*-series (A), *w*-series (B) and *q*-series (C) force and moment data. $\Delta X^+$ and $\Delta Z^+$, non-dimensional *x*- and *z*-components of the total aerodynamic force, respectively; $\Delta M^+$, non-dimensional pitching moment; $\Delta u^+$, non-dimensional *x*-components of velocity of center of mass (prefix $\Delta$ indicates that the equilibrium value is subtracted from each quantity).

Table 2. *Non-dimensional control derivatives*

| $X_\Phi^+$ | $Z_\Phi^+$ | $M_\Phi^+$ | $X_{\alpha 1}^+$ | $Z_{\alpha 1}^+$ | $M_{\alpha 1}^+$ | $X_{\bar{\phi}}^+$ | $Z_{\bar{\phi}}^+$ | $M_{\bar{\phi}}^+$ | $X_{\alpha 2}^+$ | $Z_{\alpha 2}^+$ | $M_{\alpha 2}^+$ |
|---|---|---|---|---|---|---|---|---|---|---|---|
| 0 | –2.06 | 0.03 | 0.04 | –2.91 | 0.03 | –0.19 | 0 | –3.58 | –3.08 | 0.01 | 0.53 |

$X_\Phi^+$, $Z_\Phi^+$ and $M_\Phi^+$, non-dimensional derivatives of the *x*- and *z*-component of the aerodynamic force and aerodynamic moment, respectively, with respect to the $\Phi$; $X_{\alpha 1}^+$, $Z_{\alpha 1}^+$ and $M_{\alpha 1}^+$, non-dimensional derivatives of the *x*- and *z*-component of the aerodynamic force and aerodynamic moment, respectively, with respect to $\alpha_1$; $X_{\bar{\phi}}^+$, $Z_{\bar{\phi}}^+$ and $M_{\bar{\phi}}^+$, non-dimensional derivatives of the *x*- and *z*-component of the aerodynamic force and aerodynamic moment, respectively, with respect to the $\bar{\phi}$; $X_{\alpha 2}^+$, $Z_{\alpha 2}^+$ and $M_{\alpha 2}^+$, non-dimensional derivatives of the *x*- and *z*-component of the aerodynamic force and aerodynamic moment, respectively, with respect to $\alpha_2$.

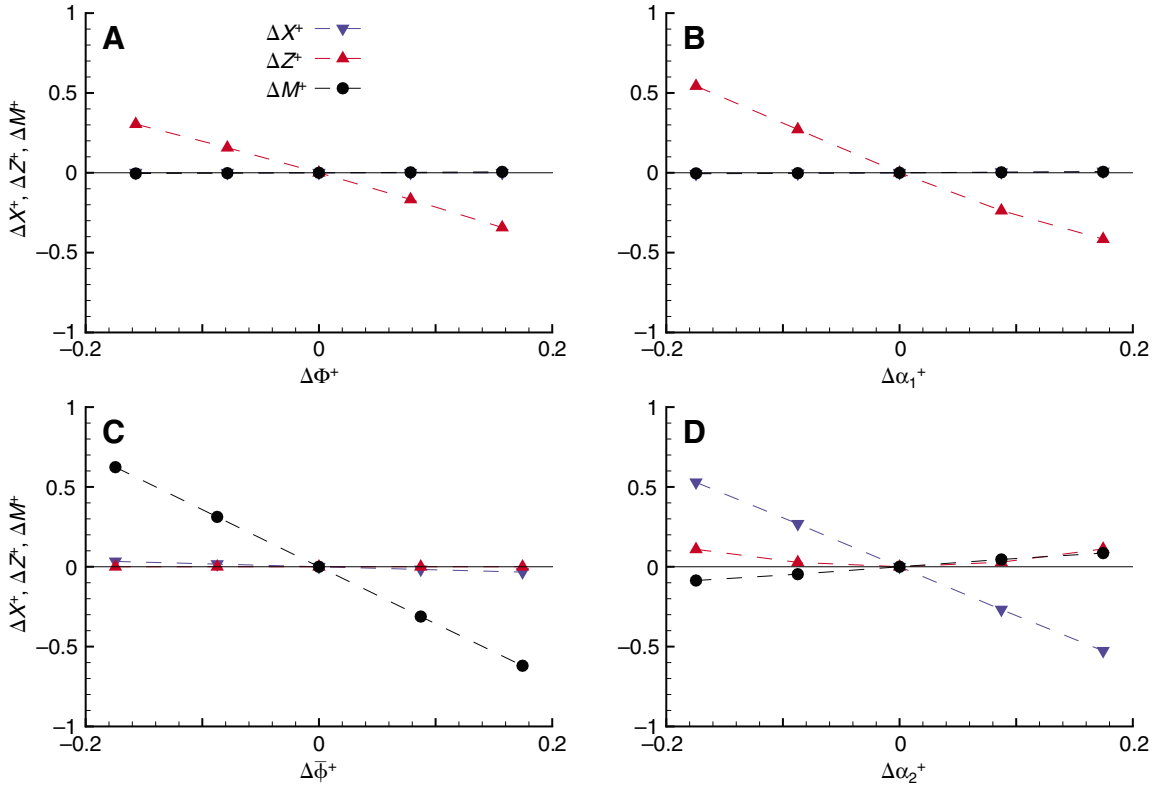


Fig. 5. The Φ-series (A), $\alpha_1$-series (B), ϕ-series (C) and $\alpha_2$-series (D) force and moment data. $\Delta X^+$ and $\Delta Z^+$, non-dimensional *x*- and *z*-components of the total aerodynamic force, respectively; $\Delta M^+$, non-dimensional pitching moment. ΔΦ and Δϕ, changes in stroke amplitude and mean stroke angle, respectively; $\Delta\alpha_1$, equal change in the down- and upstroke angles of attack; $\Delta\alpha_2$, differential change in the down- and upstroke angles of attack. Prefix Δ indicates that the equilibrium value is subtracted from the quantity.

eigenvalues of **A** and the corresponding eigenvectors, calculated in Matlab, are shown in Table 3 and Table 4, respectively. Similar to the case of the bumblebee (Sun and Xiong, 2005), there are a pair of complex eigenvalues with a positive real part and two negative real eigenvalues, representing an unstable oscillatory mode, and a stable fast subsidence mode and a slow subsidence mode, respectively. Also similar to the case of the bumblebee, the unstable oscillatory mode is a motion in which $\delta q$ and $\delta u$ are the main variables, so is the fast subsidence mode, and the slow subsidence mode is a motion in which $\delta w$ is the main variable (Table 4). The period (*T*) and the time to double ($t_{double}$) the starting value of the oscillatory mode are 43.63 and 9.37, respectively; the times to half ($t_{half}$) the starting value of the fast and low subsidence modes are 4.05 and 34.66, respectively.

### *Controllability analysis*

From the stability analysis above, we see that because of the unstable oscillatory mode, the disturbance motion is inherently unstable. For stable hovering, the model insect must apply active control. **B** in Eqn 5 is:

$$\mathbf{B} = \begin{bmatrix} 0 & 0.0006 & -0.0030 & -0.0479 \\ -0.0321 & -0.0453 & 0 & 0.0002 \\ 0.0026 & 0.0026 & -0.3073 & 0.0455 \\ 0 & 0 & 0 & 0 \end{bmatrix} \quad (6)$$

Table 3. *Eigenvalues of the system matrix*

| Mode 1 $\lambda_{1,2}$ | Mode 2 $\lambda_3$ | Mode 3 $\lambda_4$ |
|---|---|---|
| 0.074±0.144*i* | –0.171 | –0.020 |

$\lambda_{1,2}$, a pair of complex conjugate eigenvalues. $\lambda_3$ and $\lambda_4$, real eigenvalues.

(the elements of **B** are computed using the control derivatives in Table 2 and the values of $m^+$ and $I_y^+$ given above). We now apply the modal decomposition method (see e.g. Stevens and Lewis, 2003; Bryson, 1994) to the system and study its controllability properties. Let us denote the complex pair of eigenvectors corresponding to $\lambda_{1,2}$ as $\eta_1 \pm i\eta_2$, and the real eigenvectors corresponding to $\lambda_3$ and $\lambda_4$ as $\eta_3$ and $\eta_4$, respectively. Let **M** denote the eigenvector matrix of **A**:

$$\mathbf{M} = [2\eta_1 \quad 2\eta_2 \quad \eta_3 \quad \eta_4] . \quad (7)$$

Let

$$\begin{bmatrix} \delta u^+ \\ \delta w^+ \\ \delta q^+ \\ \delta\theta \end{bmatrix} = \mathbf{M} \begin{bmatrix} \xi_1 \\ \xi_2 \\ \xi_3 \\ \xi_4 \end{bmatrix}, \quad (8)$$

where $\xi_1$, $\xi_2$, $\xi_3$ and $\xi_4$ are the modal coordinates. Substituting

Table 4. *Magnitudes and phase angles of the components of each of the three eigenvectors*

| Mode | $\delta u^+$ | $\delta w^+$ | $\delta q^+$ | $\delta\theta$ |
|---|---|---|---|---|
| Unstable oscillatory | $1.3\times10^{-1}$ (125°) | $4.8\times10^{-4}$ (248°) | $1.6\times10^{-1}$ (63°) | 1 (0°) |
| Fast subsidence | $1.5\times10^{-1}$ (0°) | $6.0\times10^{-4}$ (0°) | $1.7\times10^{-1}$ (180°) | 1 (0°) |
| Slow subsidence | $3.0\times10^{0}$ (180°) | $1.4\times10^{-2}$ (0°) | $2.0\times10^{-2}$ (180°) | 1 (0°) |

$\delta u^+$, $\delta w^+$, $\delta q^+$ and $\delta\theta$, disturbance quantities in non-dimensional *x*-component and *z*-component of velocity, pitching rate and pitch angle, respectively. Numbers in the parentheses are phase angles.

Eqn 8 into Eqn 1, and then multiplying the two sides of the resulting equation by $\mathbf{M}^{-1}$, we obtain:

$$\begin{bmatrix}\dot{\xi}_1\\ \dot{\xi}_2\\ \dot{\xi}_3\\ \dot{\xi}_4\end{bmatrix} = \mathbf{A}_{nn}\begin{bmatrix}\xi_1\\ \xi_2\\ \xi_3\\ \xi_4\end{bmatrix} + \mathbf{B}_n\begin{bmatrix}\delta\Phi\\ \delta\alpha_1\\ \delta\bar{\phi}\\ \delta\alpha_2\end{bmatrix}, \quad (9)$$

where

$$\mathbf{A}_{nn} = \begin{bmatrix}0.074 & 0.144 & 0 & 0\\ -0.144 & 0.074 & 0 & 0\\ 0 & 0 & -0.171 & 0\\ 0 & 0 & 0 & -0.020\end{bmatrix}, \quad (10)$$

$$\mathbf{B}_n = \begin{bmatrix}0.003 & 0.003 & -0.289 & 0.103\\ 0.003 & 0.004 & -0.596 & -0.015\\ -0.007 & -0.006 & 0.579 & -0.207\\ 0.032 & 0.045 & 0.001 & 0\end{bmatrix}. \quad (11)$$

Eqn 9–11 are the modal form of Eqn 1. As seen in Eqn 9 and Eqn 10, $\xi_1$ and $\xi_2$ are the modal coordinates of the unsteady oscillatory mode (0.074 and ±0.144 in the first and second row of $A_{nn}$ are the real and imaginary parts of $\lambda_{1,2}$), $\xi_3$ and $\xi_4$ are the modal coordinates of the fast and slow subsidence modes (–0.171 in the third row and –0.020 in the fourth row are $\lambda_3$ and $\lambda_4$, respectively).

For stable hovering, the unstable oscillatory mode needs to be stabilized, and the slow subsidence mode needs stability augmentation (although stable, this mode converges very slowly; it needs a time of about 35 wing beats for the initial disturbance to decrease to half its initial value).

Examining Eqn 9 and Eqn 11, we note that the unsteady oscillatory mode ($\xi_1$, $\xi_2$) is well controlled by $\delta\phi$ or $\delta\alpha_2$ (in the first and second rows of $\mathbf{B}_n$, the magnitudes of the elements in the third and fourth columns are generally by two orders of magnitude larger than those in the first and second columns), and the slow subsidence mode is controllable by $\delta\Phi$ or $\delta\alpha_1$ (in the fourth row of $\mathbf{B}_n$, the magnitudes of the elements in the first and second columns are larger than those in the third and fourth columns by more than one order of magnitude).

As already shown (Table 4), the unstable oscillatory mode is a motion in which $\delta u^+$, $\delta q^+$ and $\delta\theta$ are the main variables, and the slow subsidence mode is a motion in which $\delta w^+$ is the main variable. Therefore, for the unstable oscillatory mode, quantities $\delta u^+$, $\delta q^+$ and $\delta\theta$ are observable, and for the slow subsidence mode, the quantity $\delta w^+$ is observable.

From the above analysis, we conclude that for stable hovering, the unstable oscillatory mode needs to be stabilized and the slow subsidence mode needs stability augmentation; the former can be accomplished by feeding back $\delta u^+$, $\delta q^+$ and $\delta\theta$ to produce control input $\delta\bar{\phi}$ and/or $\delta\alpha_2$ and the latter by feeding back $\delta w^+$ to produce control input $\delta\Phi$ and/or $\delta\alpha_1$.

### *Stabilization control*

Here we consider some examples where the above theory is applied and conceptually study some of the possible ways the model insect may use to stabilize its hovering flight. First, we consider a case of stabilization control using $\delta\Phi$ and $\delta\bar{\phi}$. As shown above, stabilizing the hovering flight can be accomplished by feeding back $\delta u^+$, $\delta q^+$ and $\delta\theta$ to produce $\delta\bar{\phi}$ and feeding back $\delta w^+$ to produce $\delta\Phi$. One way to realize this is to assume:

$$\delta\Phi = k_1\delta w^+, \quad (12)$$

$$\delta\bar{\phi} = k_2\delta u^+ + k_3\delta q^+ + k_4\delta\theta, \quad (13)$$

where $k_1$, $k_2$, $k_3$ and $k_4$ are constants, and choose proper values of $k_1$, $k_2$, $k_3$ and $k_4$ to obtain desired stability properties. The above analysis has shown that the slow subsidence mode mainly consists of $\delta w^+$ and is controlled by $\delta\Phi$. Thus the equation of the vertical motion can be decoupled from the first, third and fourth equations in Eqn 1, and we have:

$$\delta\dot{w}^+ = \frac{Z_w^+}{m^+}\delta w^+ + \frac{Z_\Phi^+}{m^+}\delta\Phi = -0.0196\delta w^+ - 0.0321\delta\Phi. \quad (14)$$

Substituting $\delta\Phi = k_1\delta w^+$ into Eqn 14 gives

$$\delta\dot{w}^+ = \left(\frac{Z_w^+}{m^+} + \frac{Z_\Phi^+}{m^+}k_1\right)\delta w^+ = (-0.0196 - 0.0321k_1)\delta w^+, \quad (15)$$

the eigenvalue of which is

$$\lambda_4 = -0.0196 - 0.0321k_1. \quad (16)$$

To augment the stability of this mode, the magnitude of the eigenvalue should be larger than the case of without control. Let us suppose it is desired that $\lambda_4$=–0.14 [with such a value of $\lambda_4$, the time to half the starting value of disturbance ($t_h$) is $t_h$=0.693/$|\lambda_4|\approx$5, i.e. the disturbance would decrease to half its initial value in 5 wing beats; while in the case of without control, $t_h$ is about 35]. From Eqn 16, when $k_1$ is taken as 3.751, we have $\lambda_4\approx$–0.14.

Dropping the terms containing $\delta w$ in the first, third and fourth equations of Eqn 1, we obtain the simplified equations of the unstable oscillatory and fast subsidence modes of motion:

$$\begin{bmatrix}\delta\dot{u}^+\\ \delta\dot{q}^+\\ \delta\dot{\theta}^+\end{bmatrix} = \begin{bmatrix}X_u^+/m^+ & X_q^+/m^+ & -g^+\\ M_u^+/I_y^+ & M_q^+/I_y^+ & 0\\ 0 & 1 & 0\end{bmatrix}\begin{bmatrix}\delta u^+\\ \delta q^+\\ \delta\theta\end{bmatrix} + \begin{bmatrix}X_{\bar{\phi}}^+/m^+\\ M_{\bar{\phi}}^+/I_y^+\\ 0\end{bmatrix}\delta\bar{\phi}. \quad (17)$$

Substituting Eqn 13 into Eqn 17 gives:

$$\begin{bmatrix} \delta\dot{u}^+ \\ \delta\dot{q}^+ \\ \delta\dot{\theta}^+ \end{bmatrix} = \mathbf{E} \begin{bmatrix} \delta u^+ \\ \delta q^+ \\ \delta\theta \end{bmatrix}, \quad (18)$$

where **E** is a matrix and is given as:

$$\mathbf{E} = \begin{bmatrix} -0.0199 & -0.0044 & -0.0227 \\ 0.1991 & -0.0026 & 0 \\ 0 & 1 & 0 \end{bmatrix} + \begin{bmatrix} -0.0030 \\ -0.3073 \\ 0 \end{bmatrix} [k_2 \;\; k_3 \;\; k_4] . \quad (19)$$

The characteristic equation of **E** is:

$$\lambda^3 + b\lambda^2 + c\lambda + d = 0 , \quad (20)$$

where

$$b = 0.0225 + 0.0030k_2 + 0.3073k_3 , \quad (21)$$

$$c = 0.0009 - 0.0013k_2 + 0.0067k_3 + 0.3073k_4 , \quad (22)$$

$$d = 0.0045 - 0.0070k_2 + 0.0067k_4 , \quad (23)$$

which is a cubic equation, and analytical expressions for its roots (eigenvalues $\lambda_{1,2}$ and $\lambda_3$) in terms of $k_2$, $k_3$ and $k_4$, can be obtained. In principle, given the desired eigenvalues, the values of $k_2$, $k_3$ and $k_4$ can be determined using these expressions. In practice, it is difficult to do this because these expressions are very complex. However, since the roots are known, the coefficients of Eqn 20, i.e. $b$, $c$ and $d$, can be computed using the relations between coefficients and roots ($\lambda_1+\lambda_2+\lambda_3=-b$; $\lambda_1\lambda_2+\lambda_2\lambda_3+\lambda_1\lambda_3=c$; $\lambda_1\lambda_2\lambda_3=-d$), and $k_2$, $k_3$ and $k_4$ can be easily determined by solving a set of three linear equations (i.e. Eqn 21–23). Suppose it is desired that $\lambda_{1,2}=-0.14\pm0.144i$ ($\lambda_3=-0.14$), so that the oscillatory mode becomes stable and any disturbance would decrease to half its initial value in 5 wing beats. With $b$, $c$ and $d$ computed using these values of $\lambda_{1,2}$ and $\lambda_3$, solving Eqn 21–23 gives $k_2$=0.058, $k_3$=1.293 and $k_4$=0.228.

The above results show that if the model insect uses the following controls:

$$\delta\Phi = 3.751\delta w^+ , \quad (24)$$

$$\delta\bar{\phi} = 0.058\delta u^+ + 1.293\delta q^+ + 0.228\delta\theta , \quad (25)$$

the hovering flight could be stabilized.

Similarly, it can be shown that the hovering flight could be stabilized using $\delta\alpha_1$ and $\delta\bar{\phi}$ (or $\delta\Phi$ and $\delta\alpha_2$, or $\delta\alpha_1$ and $\delta\alpha_2$).

## Discussion

### *Biological implications of the model's predictions*

The present study shows that the hovering flight of the model insect is unstable but controllable; this implies that the model insect must stabilize its flight by active control. The model predicts that the flight could be stabilized by feeding back pitch rate, pitch attitude and horizontal velocity. The sensor system of the insects must measure these feedback signals. Existing experimental data on sensor system of insects show that hoverflies and many other insects can provide those feedback signals. The pitch rate information might come from the compound eyes and also, for Diptera, from the mechanosensory halteres (e.g. Blondeau and Heisenberg, 1982; Nalbach, 1993; Dickinson, 1999; Sherman and Dickinson, 2003) [with both the compound eyes and the halteres, fruit flies could sense a wide range of angular velocity (Sherman and Dickinson, 2003)]. The pitch attitude information could be obtained by integration of the pitch rate, and for some insects might come from the ocelli, which can measure the attitude of the insect relative to the horizon (e.g. Taylor, 1981a; Taylor, 1981b; Mizunami, 1994). The horizontal velocity information might come from the compound eyes and the antennae (e.g. Borst and Egelhaaf, 1989; Dudley, 2000). The model also predicts that model insect could augment its stability by feeding back the vertical velocity. This might also come from the compound eyes and the antennae.

As observed by Ellington (Ellington, 1984b), changes in mean stroke angle and stroke amplitude, and equal and differential changes in downstroke and upstroke angles of attack of wing, are used by hoverflies and many other insects in controlled maneuvers. Here we have shown that the same control inputs, governed by different control laws, could be used to stabilize the hovering flight; i.e. for hover flight stabilization the insects do not need more control inputs than those we know empirically for maneuvers.

The predicted results that the flight is passively unstable and relies on active maintenance of stability can be advantageous to insects. It is well known that an inherently stable flying system, although it has some advantages, cannot be highly maneuverable. If the flight of an insect is inherently stable, it would not have good maneuverability that is of great importance to its survival. The present results show that when wishing to stay hovering, the insect could apply the stabilization control, and when wishing to conduct fast maneuver, it could switch off the controlled stability.

### *The stabilization control can be relatively simple and many combinations of controls can accomplish the stabilization control*

From the analysis on controllability, the stabilization control can be accomplished with only two controls: $\delta\Phi$ and $\delta\bar{\phi}$; or $\delta\alpha_1$ and $\delta\alpha_2$; or $\delta\alpha_1$ and $\delta\phi$; or $\delta\Phi$ and $\delta\alpha_2$. Furthermore, when $\delta\Phi$ and $\delta\bar{\phi}$ are used, only the fore/aft extent of the positional angle of the wing is adjusted; when $\delta\alpha_1$ and $\delta\alpha_2$ are used, only the geometrical angles of attack are adjusted. In these two cases, the control involves only one of the three angular variables of wing motion and is relatively simple.

In the above, we have listed four combinations of the controls that can accomplish the stabilization control. From the analysis on controllability, five more combinations of the controls are available for the control; they are: $\delta\Phi$, $\delta\alpha_1$ and $\delta\bar{\phi}$; $\delta\Phi$, $\delta\alpha_1$ and $\delta\alpha_2$; $\delta\Phi$, $\delta\bar{\phi}$ and $\delta\alpha_2$; $\delta\alpha_1$, $\delta\bar{\phi}$ and $\delta\alpha_2$; $\delta\Phi$, $\delta\alpha_1$, $\delta\bar{\phi}$ and $\delta\alpha_2$. That is, on the basis of controllability study, there are nine combinations of the controls available to the insect for stabilizing the hovering flight. It is reasonable to suggest that when the disturbances are relatively large, combinations with more controls may be used. For instance, when the disturbance in vertical velocity ($\delta w$) is relatively large, a combination consisted of $\delta\Phi$, $\delta\alpha_1$ and $\delta\bar{\phi}$ can be used, in which $\delta\Phi$ and $\delta\alpha_1$ are for controlling the vertical motion. Since $\delta\Phi$ and $\delta\alpha_1$ 'share' the work, they would not need to be very large and would be within their respective limits. It is of great interest to conduct some experiment to observe which combinations of the above controls are used by hoverflies and other insects that often hover

(free-flight experiments with insects who hover well could be conducted to measure the variations of wing kinematics, wing beat by wing beat, for relatively long period).

## List of symbols

| | |
|---|---|
| $\mathbf{A}$ | system matrix |
| $b$,$c$,$d$ | coefficients |
| $\mathbf{B}$ | control system matrix |
| $c$ | mean chord length |
| $\mathbf{c}$ | vector of control inputs |
| $C_H$ | horizontal force coefficient |
| $C_V$ | vertical force coefficient |
| $C_m$ | pitching moment coefficient |
| $\boldsymbol{g}$ | the gravitational acceleration |
| $i$ | imaginary number, $i=\sqrt{-1}$ |
| $I_y$ | moment of inertia about the $y$-axis of insect body |
| $l_b$ | body length |
| $k_1, k_2, k_3, k_4$ | constants |
| $l_1$ | distance from wing base axis to center of mass |
| $m$ | mass of the insect |
| $\mathbf{M}$ | eigenvector matrix of $\mathbf{A}$ |
| $M$ | total aerodynamic pitching moment about center of mass |
| $M_q$, $M_u$, $M_w$, $M_\Phi$, $M_{\alpha 1}$, $M_{\bar{\Phi}}$, $M_{\alpha 2}$ | derivative of $M$ with respect to $q$, $u$, $w$, $\Phi$, $\alpha_1$, $\bar{\Phi}$ and $\alpha_2$, respectively |
| $n$ | stroke frequency |
| $o$ | origin of coordinates $x$, $y$, $z$ |
| $q$ | pitching angular-velocity about the center of mass |
| $r_2$ | radius of the second moment of wing area |
| $R$ | wing length |
| $S$ | area of one wing |
| $S_t$ | area of two wings |
| $t$ | time |
| $t_h$ | time for a divergent motion to half in amplitude |
| $t_w$ | wing beat period |
| $T$ | period |
| $u$ | component of velocity along $x$-axis |
| $U$ | reference velocity |
| $w$ | component of velocity along $z$-axis |
| $x, y, z$ | coordinates in the body-fixed frame of reference (with origin $o$ at center of mass) |
| $x_F, y_F, z_F$ | coordinates in a system fixed on the earth |
| $X$ | $x$-component of the total aerodynamic force |
| $X_q$, $X_u$, $X_w$, $X_\Phi$, $X_{\alpha 1}$, $X_{\bar{\Phi}}$, $X_{\alpha 2}$ | derivative of $X$ with respect to $q$, $u$, $w$, $\Phi$, $\alpha_1$, $\bar{\Phi}$ and $\alpha_2$, respectively |
| $Z$ | $z$-component of the total aerodynamic force |
| $Z_q$, $Z_u$, $Z_w$, $Z_\Phi$, $Z_{\alpha 1}$, $Z_{\bar{\Phi}}$, $Z_{\alpha 2}$ | derivative of $Z$ with respect to $q$, $u$, $w$, $\Phi$, $\alpha_1$, $\bar{\Phi}$ and $\alpha_2$, respectively |
| $\alpha_1$ | equal change in geometric angle of attack |
| $\alpha_2$ | differential change in geometric angle of attack |
| $\alpha_d$ | geometric angle of attack in downstroke translation |
| $\alpha_u$ | geometric angle of attack in upstroke translation |
| $\beta$ | stroke plane angle |
| $\delta$ | small disturbance notation (prefixed to a perturbed state variable) |
| $\Delta$ | increment notation |
| $\bar{\phi}$ | mean positional angle |
| $\phi$ | positional angle |
| $\Phi$ | stroke amplitude |
| $\xi 1$, $\xi_{,2}$, $\xi_{,3}$, $\xi_{,4}$ | modal coordinates |
| $\lambda$ | generic notation for an eigenvalue |
| $\rho$ | density of fluid |
| $\theta$ | pitch angle between the $x$-axis and the horizontal |
| $\chi$ | body angle |
| $\chi_0$ | free body angle |
| Superscript + | non-dimensional quantity |

This research was supported by the National Natural Science Foundation of China.

## References

**Blondeau, J. and Heisenberg, M.** (1982). The 3-dimensional optomotor torque system of *Drosophila melanogaster* – studies on wild type and the mutant optomotor H31. *J. Comp. Physiol.* **145**, 321-329.

**Borst, A. and Egelhaaf, M.** (1989). Principles of visual motion detection. *Trends Neurosci*. **12**, 297-306.

**Bryson, A. E.** (1994). *Control of Spacecraft and Aircraft*. Princeton: Princeton University Press.

**Deng, X., Schenato, L. and Sadtry, S. S.** (2006). Flapping flight for biomimetic robotic insects. Part II, flight control design. *IEEE Trans. Rob*. **22**, 789-803.

**Dickinson, M. H.** (1999). Haltere-mediated equilibrium reflexes of the fruit fly *Drosophila melanogaster*. *Philos. Trans. R. Soc. Lond. B Biol. Sci.* **354**, 903-916.

**Dudley, R.** (2000). *The Biomechanics of Insect Flight: Form, Function, Evolution.* Princeton: Princeton University Press.

**Dudley, R. and Ellington, C. P.** (1990). Mechanics of forward flight in bumblebees. I. Kinematics and morphology. *J. Exp. Biol.* **148**, 19-52.

**Ellington, C. P.** (1984a). The aerodynamics of hovering insect flight. II. Morphological parameters. *Philos. Trans. R. Soc. Lond. B Biol. Sci.* **305**, 17-40.

**Ellington, C. P.** (1984b). The aerodynamics of hovering insect flight. III. Kinematics. *Philos. Trans. R. Soc. Lond. B Biol. Sci.* **305**, 79-113.

**Mizunami, M.** (1994). Functional diversity of neural organization in insect ocellar systems. *Vision Res*. **35**, 443-452.

**Nalbach, G.** (1993). The halteres of the blowfly *Calliphora*. I. Kinematics and dynamics. *J. Comp. Physiol. A* **173**, 293-300.

**Sherman, A. and Dickinson, M. H.** (2003). A comparison of visual and haltere-mediated equilibrium reflexes of the fruit fly *Drosophila melanogaster*. *J. Exp. Biol.* **206**, 295-302.

**Stevens, B. L. and Lewis, F. L.** (2003). *Aircraft Control and Simulation.* Hoboken, NJ: John Wiley and Sons.

**Sun, M. and Tang, J.** (2002). Unsteady aerodynamic force generation by a model fruit fly wing in flapping motion. *J. Exp. Biol.* **205**, 55-70.

**Sun, M. and Xiong, Y.** (2005). Dynamic flight stability of a hovering bumblebee. *J. Exp. Biol.* **208**, 447-459.

**Taylor, C. P.** (1981a). Contribution of compound eyes and ocelli to steering of locusts in flight. I. Behavioural analysis. *J. Exp. Biol.* **93**, 1-18.

**Taylor, C. P.** (1981b). Contribution of compound eyes and ocelli to steering of locusts in flight. II. Timing changes in flight motor units. *J. Exp. Biol.* **93**, 19-31.

**Taylor, G. K.** (2001). Mechanics and aerodynamics of insect flight control. *Biol. Rev.* **76**, 449-471.

**Taylor, G. K. and Thomas, A. L. R.** (2003). Dynamic flight stability in the desert locust *Schistocerca gregaria. J. Exp. Biol.* **206**, 2803-2829.

**Taylor, G. K., Bomphrey, R. J. and Hoen, J.** (2006). Insect flight dynamics and control. *AIAA*, 2006-32, www.aiaa.org.

**Willmott, A. P. and Ellington, C. P.** (1997). The mechanics of flight in the hawkmoth *Manduca Sexta*. I. Kinematics of hovering and forward flight. *J. Exp. Biol.* **200**, 2705-2722.